

CORRELATION COEFFICIENT IN THE CIRCULAR POLARIZATION BASIS
FOR DETECTION OF MAN-MADE TARGETS IN POLSAR IMAGE ANALYSIS

Yoshio Yamaguchi*, Koji Kimura*, Toshifumi Moriyama**, Hiroyoshi Yamada*

* Dept. of Information Engineering, Niigata University, 950-2181, Japan

** Communications Research Laboratory, Japan

Email : yamaguch@ie.niigata-u.ac.jp

1. Introduction

The purpose of this paper is to find suitable parameters for detection of man-made targets using polarimetric scattering index. The candidates of polarimetric indices are total power, scattering matrix elements, polarization signature, coherency vector, polarimetric entropy, angle alpha, anisotropy, eigenvalue, correlation coefficient, etc. Among them, we focus our attention to the correlation coefficient because it is one of essential tools not only for polarimetric SAR image analysis but also for statistical image analysis. Even if we apply the correlation coefficient to fully polarimetric SAR image, there will be variations according to the combination of polarization index.

2. Correlation Coefficient

Polarimetric SAR image consists of thousands of pixels. Each pixel corresponds to a scattering matrix

$$[S(HV)] = \begin{bmatrix} S_{HH} & S_{HV} \\ S_{VH} & S_{VV} \end{bmatrix}. \tag{1}$$

The scattering matrix is acquired with fully polarimetric SAR system such as Pi-SAR, AIRSAR, and E-SAR. Since we can assume $S_{HV} = S_{VH}$ for monostatic radar system, we have 3 complex independent values (S_{HH} , S_{HV} , and S_{VV}). We use the second-order statistics of the scattering matrix for the image analysis.

In general, the correlation coefficient is defined as

$$\gamma_{AB-XY} = \frac{\langle S_{AB} S_{XY}^* \rangle}{\sqrt{\langle S_{AB} S_{AB}^* \rangle \langle S_{XY} S_{XY}^* \rangle}} = |\gamma_{AB-XY}| \exp(j \phi_{AB-XY}), \tag{2}$$

where $\langle \bullet \rangle$ indicates ensemble average, and the subscripts A, B, X, and Y are polarization indices such as H (horizontal), V (vertical), etc. These indices can be chosen arbitrarily because of the polarization basis transformation. Typical correlation coefficients in polarimetric SAR image analysis are,

(a) the HV polarization basis:

$$\gamma_{HH-HV} = \frac{\langle S_{HH} S_{HV}^* \rangle}{\sqrt{\langle S_{HH} S_{HH}^* \rangle \langle S_{HV} S_{HV}^* \rangle}} = |\gamma_{HH-HV}| \exp(j\phi_{HH-HV}), \quad (3)$$

(b) the 45 -135 degree oriented linear polarization basis with $X=45^\circ$, $Y=135^\circ$:

$$\gamma_{XX-YY} = \frac{\langle S_{XX} S_{YY}^* \rangle}{\sqrt{\langle S_{XX} S_{XX}^* \rangle \langle S_{YY} S_{YY}^* \rangle}} = |\gamma_{XX-YY}| \exp(j\phi_{XX-YY}). \quad (4)$$

(c) the circular polarization basis with R (right circular pol.) and L (left circular pol.):

$$\gamma_{RR-LL} = \frac{\langle S_{RR} S_{LL}^* \rangle}{\sqrt{\langle S_{RR} S_{RR}^* \rangle \langle S_{LL} S_{LL}^* \rangle}} = |\gamma_{RR-LL}| \exp(j\phi_{RR-LL}), \quad (5)$$

It is known for natural distributed targets with reflection symmetry that $\langle S_{HH} S_{HV}^* \rangle \approx 0$, $\langle S_{VV} S_{HV}^* \rangle \approx 0$ and hence $|\gamma_{HH-HV}| \approx 0$, and that the phase angle ϕ_{HH-HV} is uniformly distributed in $[0, 2\pi]$. This property applies to microwave frequency bands. Under the condition $\langle S_{HH} S_{HV}^* \rangle \approx 0$ and $\langle S_{VV} S_{HV}^* \rangle \approx 0$, the correlation coefficient in the circular polarization basis can be approximated as,

$$\gamma_{RR-LL} = \frac{\langle 4 |S_{HV}|^2 - |S_{HH} - S_{VV}|^2 \rangle}{\langle 4 |S_{HV}|^2 + |S_{HH} - S_{VV}|^2 \rangle}, \quad (6)$$

It should be noted in (6) that γ_{RR-LL} is real-valued, and that the phase ϕ_{RR-LL} is 0 or π depending on the magnitude balance between $4 |S_{HV}|^2$ and $|S_{HH} - S_{VV}|^2$. This means, if γ_{RR-LL} after the calculation of (5) becomes a complex value with the phase different from 0 or π , the corresponding area contains non-natural distributed targets, i.e., some man-made targets. This is the main topic of this manuscript. The conditions $\langle S_{HH} S_{HV}^* \rangle \approx 0$ and $\langle S_{VV} S_{HV}^* \rangle \approx 0$ are incorporated into the phase angle expression,

$$\phi_{RR-LL} = \tan^{-1} \frac{\langle \text{Re} \{ 4 S_{HV}^* (S_{HH} - S_{VV}) \} \rangle}{\langle 4 |S_{HV}|^2 - |S_{HH} - S_{VV}|^2 \rangle} \quad (7)$$

This phase angle ϕ_{RR-LL} provides $\sin \phi_{RR-LL} \approx 0$ for natural distributed targets, and $\sin \phi_{RR-LL} \neq 0$ for non-natural targets (man made targets). The restriction imposed on $\text{Re} \{ 4 S_{HV}^* (S_{HH} - S_{VV}) \} \neq 0$ indicates highly complex scattering nature (rotation symmetry) because there exists no canonical basic targets such as sphere, diplane, or helix. Therefore, this condition is one of indicators for complex target. In addition, the magnitude balance between $4 |S_{HV}|^2$ and $|S_{HH} - S_{VV}|^2$ is sensitive to target nature.

In the $45^\circ - 135^\circ$ linear polarization case, we have

$$\gamma_{XX-YY} = \frac{\left\langle \left| S_{HH} + S_{VV} \right|^2 - 4 \left| S_{HV} \right|^2 \right\rangle}{\left\langle \left| S_{HH} + S_{VV} \right|^2 + 4 \left| S_{HV} \right|^2 \right\rangle}. \quad (8)$$

Since $\left| S_{HH} + S_{VV} \right|^2 > 4 \left| S_{HV} \right|^2$ applies to most of targets, the value becomes positive and the phase ϕ_{XX-YY} is 0 degree for natural distributed target.

It is expected from the consideration on scattering characteristics that ϕ_{RR-LL} and $\left| \gamma_{RR-LL} \right|$ are sensitive indices rather than $\left| \gamma_{HH-HV} \right|$ or γ_{XX-YY} for distinguishing between natural and non-natural complex targets. It is interesting to note that γ_{RR-LL} is mainly composed of target vector components $S_{HH} + S_{VV}$, $S_{HH} - S_{VV}$, and $2S_{HV}$.

3. X-band Pi-SAR Image

It is well known that building wall whose normal direction is not parallel to radar illumination exhibits small RCS, and that the cross polarized HV component from these buildings is rather dominant. On the other hand, buildings whose wall normal is parallel to radar illumination reflects large double bounce component. Thus the SAR image of buildings becomes green (color representation of HV component) or bright red (double bounce component representation) depending on the directions of building wall with respect to radar illumination or SAR flight path. If buildings are surrounded by trees or vegetation (which also exhibits small RCS with co- and cross-polarized component, and little contribution of double bounce), the detection of buildings in vegetation area becomes quite difficult.

We applied $\sin \phi_{RR-LL}$ for detection of man-made target including buildings, because building is one of the typical man-made targets. Fig.1 shows a polarimetric SAR image around Niigata University which has been acquired with Pi-SAR airborne system (CRL/NASDA, X-band, data no.6012). The image is based on the target vector components, i.e., $2 \left| S_{HV} \right|$ (green), $\left| S_{HH} - S_{VV} \right|$ (red), and $\left| S_{HH} + S_{VV} \right|$ (blue) components corresponding to cross pol generation, double bounce, and single bounce, respectively. The scene contains large buildings, residential area, the Sea of Japan, the Shinkawa river, crop fields, and pine woods. The residential area and buildings are aligned non parallel to SAR flight path. It is seen that the cross-polarized component highly contributes to backscattering from oriented buildings. The backscattering characteristics in residential area are similar to those in vegetated area. Although the pixel resolution of Pi-SAR image is fine with 1.5 m by 1.5 m on the ground, we tried a 9 by 9 pixel averaging window to obtain correlations based on the statistics and examined the availability of ϕ_{RR-LL} for detection of oriented buildings and man made targets.

Fig. 2 overlays the phase information ϕ_{RR-LL} on Fig.1. The range $-\frac{3}{4}\pi < \phi_{RR-LL} < \frac{3}{4}\pi$ is picked up and is colored white in order to distinguish $\phi_{RR-LL} \approx \pi$ for vegetation area. It is seen that buildings and residential houses are well detected. This shows a promising result and good correlation with Fig.1.

For quantitative analysis, the value of $\sin \phi_{RR-LL}$ is plotted in Fig.3 along lines A and B in Fig.1. The region corresponding to specific area are shown for the correspondence. As is seen from the figure, $\sin \phi_{RR-LL}$ supports the validity of the method.

4. Conclusion

The phase angle of correlation coefficient in the circular polarization basis is proposed to discriminate natural distributed target versus non-natural target. The X-band Pi-SAR data shows that the phase angle is useful for distinguishing between natural and non-natural distributed targets. This method also serves to detect complex urban area containing buildings or houses aligned not parallel to SAR flight path.

ACKNOWLEDGMENTS

The authors would like to thank NASDA, and CRL for providing valuable Pi-SAR image data sets. This work in part was supported by Grant in Aid for Scientific Research, JSPS, Japan.

REFERENCES

- [1] A. Freeman, and S. Durden, "A three-component scattering model for polarimetric SAR data," *IEEE Trans. Geosci. Remote Sensing*, vol. 36, no. 3, pp. 963-973, May 1998.
- [2] J. S. Lee, D. L. Schuler, and T. L. Anisoworth, "Polarimetric SAR data compensation for terrain azimuth slope variations," *IEEE Trans. Geosci. Remote Sensing*, vol.38, no.5, pp.2153-2163, 2000.
- [3] M. Murase, Y. Yamaguchi, and H. Yamada, "Polarimetric correlation coefficient applied to tree classification," *IEICE Trans. Commun.*, vol. E84-B, no. 12, pp. 1835-1840, Dec. 2001.

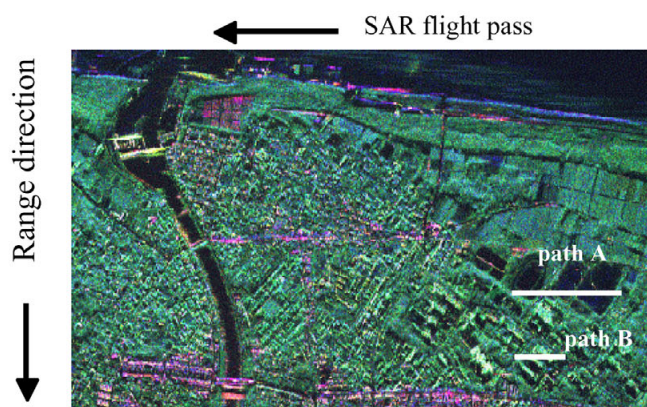


Fig.1 Pi-SAR X-band color composite image with $2|S_{HV}|$ (green), $|S_{HH} - S_{VV}|$ (red), and $|S_{HH} + S_{VV}|$ (blue)

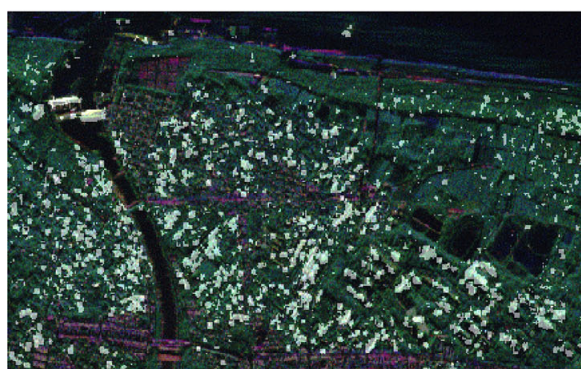
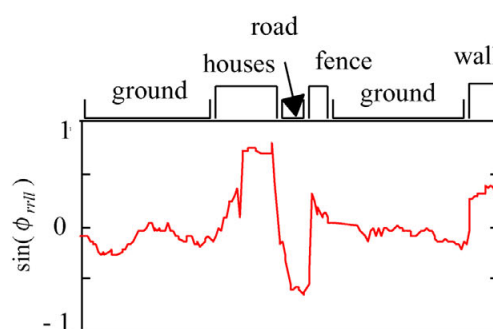
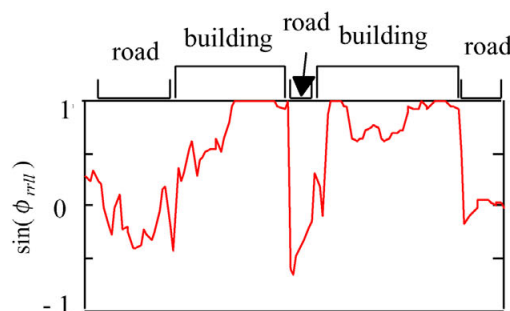


Fig. 2 Phase overlay image larger than on Fig.1



(a)

Fig.3 Phase information along path A



(b)

Fig.3 Phase information along path B